Modeling and analysis of finite phased arrays of microstrip antennas : an eigenvector approach

Modeling and Analysis of Finite Phased Arrays of Microstrip Antennas - An Eigenvector Approach

D. J. Bekers S. J. L. van Eijndhoven A. A. F. van de Ven*
P-P. Borsboom† A. G. Tijhuis ‡

Abstract — **In this paper, a model is developed to determine characteristics of finite phased arrays of microstrip antennas. This model concerns a finite array of simple elements: perfectly conducting, infinitely thin, narrow rings, excited by voltage gaps and positioned in free or above a ground plate. The currents on the rings, and from that the electromagnetic field, are calculated by a moment method. Dimension analysis is carried out to reduce numerical effort and to acquire insight in the array behaviour. The first step is made towards determining the array characteristics by linking the eigenvalue behaviour of the moment impedance matrix to mutual coupling.**

1 INTRODUCTION

Recently Thales Nederland has realized new radar systems consisting of large phased arrays of microstrip antennas. The arrays consist of about 1000 rectangular microstrip loops, positioned on an antenna face of about $16\,\mathrm{m}^2$. The systems scan in azimuth by rotation and in elevation by phase shifts.

For analysis and design of such arrays, infinite array models are used, but these models cannot account for edge effects and differences between antenna elements. Therefore, there is need for a finite array model that can also provide insight in the characteristics describing the qualitative behaviour of large phased arrays. Characteristics should relate the array geometry to typical parameters, like side lobe level, gain, and scattering parameters. Simulation of a finite array taking into account the complex antenna element geometry requires unrealistic computing time. Hence, we have developed a model based on simple elements to find the characteristics. In this way, we hope to find underlying structures that will decrease computation times drastically for more realistic configurations.

In this paper, we show the modeling and analysis aspects of finite arrays of one specific element. Moreover, we present the first step towards determining characteristics of such arrays. This step is based on relating the eigenvalue behaviour of the impedance operator to mutual coupling aspects.

2 MODELING AND ANALYTICAL ASPECTS

We choose annular-shaped microstrips, or rings, as elements, which are infinitely thin and perfectly conducting. Reasons for this choice are twofold. Firstly, a ring is the most simple loop geometry to be described mathematically and secondly, the modes on this geometry can be described analytically. The ring widths $2b_q$ are much smaller than the wavelength, the ring circumferences $2\pi a_q$, and the distances between the rings. In other words, $kb_q \ll 1$, $\beta_q = b_q/a_q \ll 1$, and $b_p/(|\mathbf{c}_p - \mathbf{c}_q| - a_p - a_q) \ll 1$, see Figure 1. The current can be then averaged with respect to the ring widths and its component perpendicular to the centerlines of the rings can be neglected. The arrays are planar positioned in free space or above an infinitely wide ground plate, see Figure 2. Arbitrary sub-collections of rings are excited at a certain frequency, with corresponding wavelength λ and wave number k, by a prescribed tangential excitation field on the rings

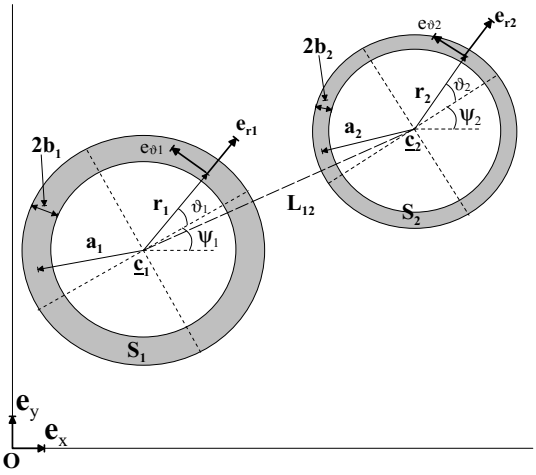

Figure 1: Two rings and their corresponding geometry parameters and local coordinate systems.

*Department of Mathematics and Computing Science, Eindhoven University of Technology, P.O. Box 513, 5600 MB, Eindhoven, The Netherlands, e-mail: d.j.bekers@tue.nl

†Department JRS-TU Antenna, Thales Nederland, P.O. Box 40, 7550 GD, The Netherlands

‡Department of Electrical Engineering, Eindhoven University of Technology, P.O. Box 513, 5600 MB, Eindhoven, The Netherlands

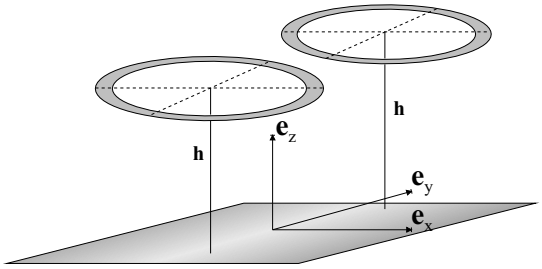

Figure 2: Geometry of an array of two rings above a ground plate.

originating from external sources (planar waves) or local feeds (delta gaps, finite voltage jumps, proximity coupled small rings). The local feeds can be positioned arbitrarily on or near the rings.

A spatial time-harmonic representation of the electromagnetic (EM) fields is used. The tangential excitation field $(\mathbf{E}^{ex})_{tan}$ is related to the current $\mathbf{J}$ by the so-called (infinite dimensional) impedance operator consisting of an integro-differential operator $\mathcal{L}$ and a trace operator $(\,\cdot\,)_{tan}$. The integral operator, described by a Green's kernel, relates the magnetic vector potential to the current, and the differential operator relates the scattered electric field to the magnetic vector potential. The trace operator restricts a vector field to the surface S of the rings and takes its tangential component. The resulting equation, i.e.

$$(\mathcal{L}\mathbf{J})_{tan} = -(\mathbf{E}^{ex})_{tan}, \qquad \text{on } S, \tag{1}$$

is tackled by a moment method, expanding the current into a finite number of expansion functions. Knowing the current, the EM far field is determined analytically.

On each ring surface S_q a parameter representation described by an angle ψ_q is chosen, see Figure 1, which can be extended straightforwardly to a global coordinate system. As aforementioned, the current $\mathbf{J}$ is averaged with respect to the widths $2b_q$ of the rings and directed along their center lines, $\mathbf{J}|_{S_q}(r_q, \vartheta_q) = w_q(\vartheta_q)\mathbf{e}_{\vartheta_q}$. Based on dimension analysis of $(\mathcal{L}\,\cdot)_{tan}$, the test functions used in the moment impedance matrix calculation are averaged with respect to the ring widths. Test functions with only tangential components on the rings are chosen. By this procedure, the Green's kernel is averaged with respect to the local radial coordinates on the rings, resulting in an adjusted integral operator with logarithmic singular kernel and an adjusted differential operator. Moreover, the moment impedance matrix components reduce to double and single integrals in case of mutual- and self-coupling, respectively. The expansion and test functions are chosen as eigenfunctions of the Sturm-Liouville, or Helmholtz, part of the differential operator resulting in entire domain functions of sine or cosine type, i.e. $w_q(\vartheta_q) = \cos n\vartheta_q$ and $w_q(\vartheta_q) = \sin n\vartheta_q$. The numbers of expansion functions $N_{cos,q}$ and $N_{sin,q}$ can differ per ring. The resultant matrix equation $ZI = V$ for the expansion coefficients I is solved by LU-decomposition. The moment impedance matrix is a diagonal dominant block matrix, each block representing the interaction of test and expansion functions defined on specific rings. The diagonal and off-diagonal blocks are diagonal and dense matrices, respectively. More details of the analysis are described in [1].

3 RELATIONS BETWEEN EIGENVALUES AND MUTUAL COUPLING

The described method in itself provides little physical insight and is computationally intensive for large arrays. Since we seek characteristics of arrays, we express the current on the rings as a linear combination of the eigenvectors U_n of the moment impedance matrix, the coefficients being the inverted eigenvalues ν_n,

$$I = \sum_{n=1}^{N} \frac{X_n}{\nu_n} U_n \,. \tag{2}$$

Here, the coefficients X_n depend on the level of orthogonality of the eigenvectors described by their Gramm matrix. For orthonormal eigenvectors, $X_n = (V \bullet U_n)$, where $(\,.\bullet.\,)$ is the Euclidean inner product. The eigenvalues ν_n are the same as the eigenvalues of the corresponding averaged finite dimensional impedance operator resulting from the asymptotic analysis of $(\mathcal{L}\,\cdot)_{tan}$ mentioned above. The eigenvectors U_n are one-to-one related to the eigenfunctions of this operator. The components of each U_n are the expansion coefficients of such an eigenfunction with respect to the finite basis of the expansion functions. Each eigenfunction represents an eigencurrent of the array.

The eigenvalues ν_n of a solitaire ring are found as the diagonal components of the moment impedance matrix Z. Each ν_n belongs to exactly one expansion (eigen)function $\cos\zeta(n)\vartheta$ or $\sin\zeta(n)\vartheta$. Moreover, cosine and sine expansion functions of equal 'frequency' n have equal eigenvalues.

For arrays with uniform (but variable) ring geometry, the eigenvalues of arrays can be divided into groups such that each group relates to an eigenvalue of a solitaire ring. The corresponding (non-orthogonal) eigenvectors are perturbed with respect to the (orthogonal) eigenvectors of the same array

in which mutual coupling is disregarded. For a fixed number of rings, the spread of the eigenvalues in each group is a measure of mutual coupling between the eigenvectors, or eigencurrents, in the groups. A large spread corresponds to a high degree of mutual coupling, whereas a small spread corresponds to a low degree. For arrays with a uniform number of expansion functions, each group consists of N_r eigenvalues, where N_r is the number of rings.

4 NUMERICAL RESULTS

Validation of the implementation of the presented model for arrays of rings has been described in [1]. Here, we describe results of the eigenvalue and eigenvector analysis of the previous section. First, we consider the behaviour of the eigenvalues of a solitaire ring, which we order ascendingly. Figure 3 and 4 show this behaviour for several values of ka and several values of h/λ. For

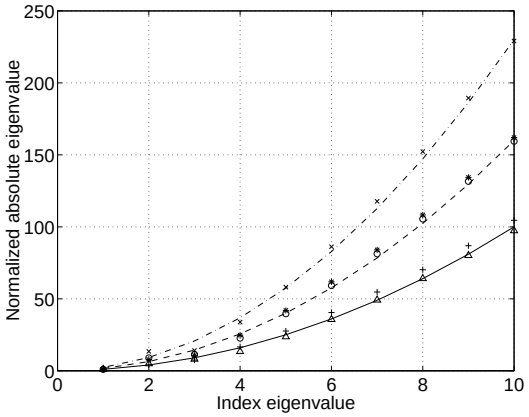

Figure 3: First 10 eigenvalues, normalized on the smallest eigenvalue, of a solitaire ring in free space as function of their indices for several values of ka; $+:\ ka = 0.838$, $*:\ ka = 0.942$, $\times:\ ka = 1.047$, $\circ:\ ka = 1.152$, $\triangle:\ ka = 1.257$. Other parameters: $b/\lambda = 0.005$, $N_{cos} = 10$, $N_{sin} = 0$. Solid line: $y = x^2$, dashed line: $y = 8x^2/5$, dashed-dotted line: $y = 23x^2/10$.

all results, the eigenvalues ν_n correspond to the expansion functions with 'frequency' $\zeta(n)$, where $\zeta = (1, 2, 0, 3, 4, 5, ...)$. Both figures show that the eigenvalues ν_n tend as n^2 for $n \leq 10$, which is the same behaviour as the eigenvalues of the Helmholtz operator exhibit. This implies that the Helmholtz part of the (averaged) differential operator dominates the (averaged) integral operator with logarithmic singular kernel. For $n > 10$, this dominance loses strength; the eigenvalues tend as $n\sqrt{n}$. However, this behaviour is of lesser importance, because the current in (2) will be described by the first few

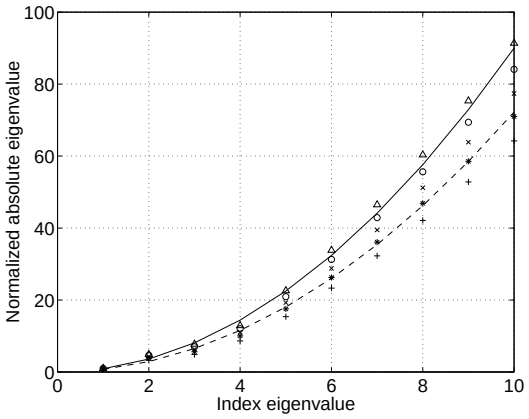

Figure 4: First 10 eigenvalues, normalized on the smallest eigenvalue, of a solitaire ring in half space as function of their indices for several values of h/λ; $+:\ h/\lambda = 0.1$, $*:\ h/\lambda = 0.15$, $\times:\ h/\lambda = 0.2$, $\circ:\ h/\lambda = 0.25$, $\triangle:\ h/\lambda = 0.3$. Other parameters: $ka = 1.257$, $b/\lambda = 0.005$, $N_{cos} = 10$, $N_{sin} = 0$. Solid line: $y = 9x^2/10$, dashed line: $y = 13x^2/18$.

terms of the series due to the quadratic behaviour of the eigenvalues for $n \leq 10$.

To investigate how many expansion functions we need to obtain accurate results for the first M eigenvalues, we have carried out numerical tests for several geometries of N_r rings, $N_r = 1, 2, 10, 20, 40, 60$. Uniform but variable numbers of cosine expansion functions are prescribed on the rings. The results show that for $N_{cos} \geq 3$, all $M = N_r N_{cos}$ eigenvalues are determined up to 0.5%.

Finally, we study the spread of the inverted eigenvalues in each of the groups for several array geometries. Figure 5 shows the maximum and minimum absolute inverted eigenvalues of the four eigenvalue groups of line arrays of $2, 4, ..., 60$ rings with uniform spacing $3\lambda/5$. The arrays have uniform ring geometry and a uniform number of expansion functions per ring. We observe that the first group has the largest spread for all numbers of rings, followed by the third group. The other two groups have a much smaller spread. Hence, mutual coupling effects are mainly incorporated in the 1st and 3rd group. In half space, we observe similar behaviour, see Figure 6, but now the 3rd group has the largest spread for all numbers of rings, followed by the 1st group. Again the other two groups have much smaller spread. Moreover, groups with higher group number n, which appear for larger numbers of expansion functions, will also have much smaller spread, because the spread decreases as n increases. Therefore, mutual coupling is mainly described by the first and the third group of eigenva-

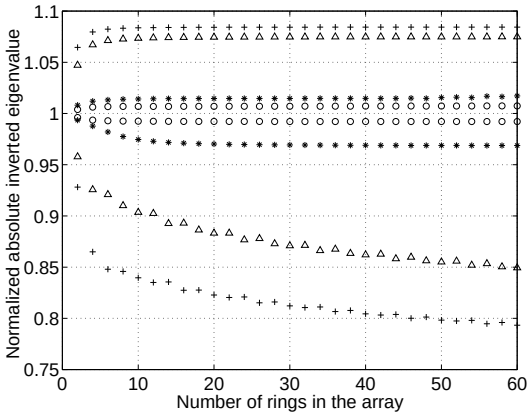

Figure 5: Maximum and minimum absolute inverted eigenvalues of the four eigenvalue groups of line arrays of $2, 4, ..., 60$ rings in free space with spacing $3\lambda/5$; $+$: 1st group, $*$: 2nd group, $\triangle$: 3rd group, $\circ$: 4th group. Other parameters: $ka_q = 2\pi/5$, $\beta_q = 1/40$, $\psi_q = 0$, $N_{cos,q} = 4$, $N_{sin,q} = 0$.

lues and eigenvectors. These groups correspond to the eigenvalues of one ring with cosine eigenfunctions of 'frequency' $\zeta(1) = 1$ and $\zeta(3) = 0$. Due to the quadratic behaviour of the eigenvalues, the mutual coupling incorporated in the first group will be of more importance for determining the current I than the third group.

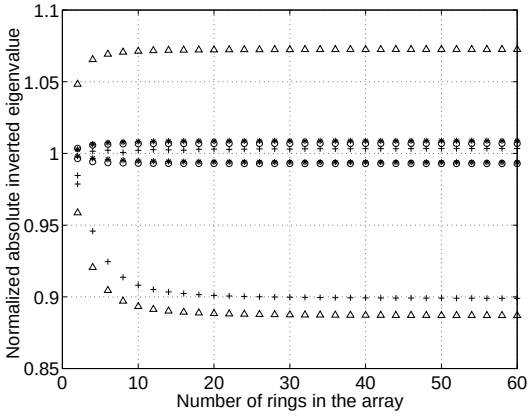

Figure 6: Maximum and minimum absolute inverted eigenvalues of the four eigenvalue groups of line arrays of $2, 4, ..., 60$ rings in half space with spacing $3\lambda/5$; $+$: 1st group, $*$: 2nd group, $\triangle$: 3rd group, $\circ$: 4th group. Other parameters: $ka_q = 2\pi/5$, $\beta_q = 1/40$, $\psi_q = 0$, $h = \lambda/4$, $N_{cos,q} = 4$, $N_{sin,q} = 0$.

For line arrays with uniform but variable spacing, ring geometry, and number of expansion functions, as we have considered, the moment impedance matrix Z is of block Toeplitz type, see [2]. The numerical convergence of the upper bounds of each of the groups and the numerical divergence of some of the lower bounds can be related to theorems in [2, Ch. 4, 6] on the singular values of block Toeplitz matrices. The divergent lower bounds indicates that the Fourier series induced by the block Toeplitz matrix is not bounded, see [2, Sec. 4.4, 6.4].

The CPU times of a Matlab implementation on a HP PC with Windows NT, an Intel Pentium IV processor at 1.0 GHz, and 256 Mb of RAM are 2 min. 36 sec. and 38 min. for constructing Z of arrays of 10 and 40 rings with 8 expansion functions. For 4 expansion functions, these times are only 17.1 sec. and 3 min. 45 sec. If the Toeplitz structure of Z is used for line arrays, then the CPU times for 8 expansion functions reduce to 12.3 sec. and 1 min. 47 sec. Note that the CPU time for constructing Z dominates the total CPU time for solving $ZI = V$; inversion of Z requires in all aforementioned cases less than 1 sec.

5 CONCLUSIONS

We have developed a tool for analyzing finite arrays of rings, or more specifically, for determining the characteristics of such arrays. A first step towards this determination has been made by linking mutual coupling to the behaviour of the eigenvalues of the moment impedance matrix.

6 PROSPECTS

A more detailed study of the eigenvalues and their relation to mutual coupling is still in progress. Moreover, the behaviour of the eigenvectors will be topic of further research. An approximation technique is under development to calculate the eigenvectors of an array with mutual coupling from the eigenvectors of the same array in which mutual coupling is disregarded. By this technique, computational effort should be reduced further, also for more realistic configurations.

References

[1] D.J. Bekers and S.J.L. van Eijndhoven and A.A.F. van de Ven and P-P. Borsboom and E.W. Kolk, "Finitely Large Phased Arrays of Microstrip Antennas - Analysis and Design", Proceedings SCEE 2002, Eindhoven (The Netherlands), to be published (also at: http://www.win.tue.nl/analysis/preprints/).

[2] A. Böttcher and B. Silbermann, "Introduction to Large Truncated Toeplitz Matrices", Springer, New York, 1999.